

Narrow-linewidth 1944 nm DBR laser based on a Tm: YAG-crystal-derived silica fiber measured by a Brillouin/thulium fiber laser beat-frequency technique

Ling Yang (杨玲)¹, Jianxiang Wen (文建湘)^{1*}, Jun Hu (胡君)¹, Liang Zhang (张亮)¹, Zhiying Luo (骆志颖)², Jingshen Zhang (张敬申)², Chengwu Yang (杨成武)², Fufei Pang (庞拂飞)¹, and Tingyun Wang (王廷云)¹

¹Key Lab of Specialty Fiber Optics and Optical Access Networks, Joint International Research Laboratory of Specialty Fiber Optics and Advanced Communication, School of Communication and Information Engineering, Shanghai University, Shanghai 200444, China

²Shanghai Raykeen Laser Technology Co., Ltd., Shanghai 201201, China

*Corresponding author: wenjx@shu.edu.cn

Received April 21, 2025 | Accepted July 23, 2025 | Posted Online November 7, 2025

An all-fiber single-frequency distributed Bragg reflector (DBR) laser at 1944 nm was demonstrated using a 2-cm-long home-made Tm-doped yttrium aluminum garnet (YAG)-crystal-derived silica fiber (TYDSF). The laser delivered stable single-transverse and longitudinal-mode operation with an output power of 226 mW, achieving a slope efficiency of 38.83%, an optical signal-to-noise ratio of >81 dB, a pump threshold as low as 21 mW, and power fluctuations <0.27% over 10 h. To the best of our knowledge, a beat-frequency technique based on a single-frequency Brillouin/thulium fiber laser was employed to characterize the 2 μm band laser linewidths for the first time, achieving a narrowed linewidth of 9.25 kHz via a passive optical feedback loop. These results underscore the laser's potential as a robust seed source for medical surgery, atmospheric monitoring, and mid-infrared coherent communications.

Keywords: single-frequency fiber laser; Tm: YAG-crystal-derived fiber; Brillouin/thulium fiber laser; linewidth characterization.

DOI: [10.3788/COL202523.121402](https://doi.org/10.3788/COL202523.121402)

1. Introduction

With the characteristics of eye-safety, low atmospheric transmission loss, narrow linewidth, and low intensity noise, single-frequency fiber lasers (SFFLs) operating at 2 μm have garnered significant interest for applications in atmospheric detection, satellite remote sensing, coherent Doppler lidar, and non-invasive medicine^[1–5]. Diverse cavity configurations, including a distributed Bragg reflector (DBR)^[6], distributed feedback (DFB)^[7] cavities, long linear cavities^[8], and traveling-wave ring cavities^[9,10], have been explored to achieve single-longitudinal-mode (SLM) operation in fiber lasers. In the DBR cavity, a pair of Bragg gratings is spliced to both ends of the gain fiber, achieving a compact cavity length of several centimeters with GHz-level longitudinal mode spacing. This design ensures stable SLM operation while offering enhanced structural compactness and superior slope efficiency^[11]. But the ultra-short cavity critically depends on high-gain active fibers to achieve high-efficiency SFFLs. Recent advances in fiber materials have introduced novel platforms enabling high-concentration doping of rare-earth ions, including tellurate fibers^[12], germanate

fibers^[13], and crystal-derived silica fibers^[14–18]. Among these, YAG-crystal-derived silica fibers (YDSFs), featuring yttrium aluminosilicate glass cores, are promising for linear-cavity fiber lasers due to their exceptional compatibility with commercial silica fibers, excellent mechanical properties, thermal stability, and high-rare-earth-ion doping concentrations^[14,15].

In 2023, Wei *et al.* demonstrated a DBR SFFL based on a Tm: YAG/Ho: YAG crystal fiber with a slope efficiency of 29.68% and a linewidth of 23.65 kHz^[16]. Later in 2025, the group developed a 1941 nm SFFL based on a Tm: YAG-crystal-derived silica fiber (TYDSF), achieving a slope efficiency of 50.83%, an optical signal-to-noise ratio (OSNR) exceeding 66.5 dB, and a linewidth of 40.75 kHz^[18]. Both laser linewidth characterizations employed the delayed self-heterodyne (DSH) method, which exhibits significant inaccuracies due to the limited fiber delay line length caused by the high transmission loss (~ 20 dB/km) of 2 μm band lasers in single-mode fibers (SMFs). Moreover, an imbalanced Michelson interferometer with a 3×3 coupler was utilized to measure the power spectral density of phase noise for linewidth determination^[19,20]. However, the method requires complex system configurations and data processing procedures, while

the stringent environmental stability requirements imposed by active feedback control further challenge its practical implementation. A single-frequency Brillouin/thulium fiber laser (BTFL) exhibits a low Brillouin pump threshold, narrow linewidth, and a Brillouin frequency shift^[21–23], making it an ideal reference source. The BTFL-based beat-frequency technique is promising for 2 μm band laser linewidth characterization, offering simplified implementation with inherent immunity to laser wavelength variations.

In this work, the TYDSFs were fabricated with a Tm: YAG crystal rod, and based on the TYDSF, a high-OSNR DBR SFFL was constructed. The laser characteristics were systematically analyzed, encompassing transverse and longitudinal mode behavior, power stability, relative intensity noise (RIN), and so on. Furthermore, a passive optical feedback loop was used to narrow the linewidth of the SFFL, and to the best of our knowledge, a BTFL was constructed with the beat-frequency technique to characterize the linewidth for the first time.

2. Fiber Characterization and Laser Configuration

The TYDSF samples were fabricated via a melt-in-tube method using a CO₂-laser-heating drawing tower at $\sim 2100^\circ\text{C}$, with preforms consisting of 15.0 at. % Tm: YAG crystal rods and high-purity silica tubes. Cross-sectional energy dispersive X-ray spectroscopy (EDS, Thermo Scientific, USA) analysis revealed abrupt elemental transitions at core/cladding interfaces [see Fig. 1(a)], demonstrating Si diffusion from cladding to core. The amounts of Y, Al, and Tm in the core are 19.58% (mass fraction), 10.49% (mass fraction), and 2.30% (mass fraction), respectively. The Tm element is uniformly distributed in the fiber core. The refractive index distribution of the TYDSF, as shown in Fig. 1(b), was measured by a fiber refractive index analyzer (S14, Photon Kinetics Inc., USA). The calculated numerical aperture was approximately 0.35. Microscopic examination confirmed a well-defined waveguide structure, exhibiting core/cladding diameters of 14.6/126.0 μm .

The absorption spectrum of the fabricated TYDSF was measured with a back-cutting method using a broadband source (BBS, NKT Photonics, Denmark) and an optical spectrum analyzer (OSA, AQ6375, YOKOGAWA, Japan) as depicted in Fig. 1(c). The typical absorption peaks of Tm³⁺ ions exist at 786.3, 1210.1, and ~ 1610 nm bands, the absorption coefficients of which are respectively 4.02, 3.27, and 2.00 dB/cm. Figure 1(d) displays the transmission loss of the TYDSF with a back-cutting method, which is determined to be 2.708 dB/m at 1310 nm. The unsaturated absorption characteristic is determined by the properties of the fiber material, which describes the process in which pump photons are absorbed^[24]. In Fig. 1(e), the saturated and unsaturated absorption coefficients (α_s and α_{us}) are 1.37 and 0.13 dB/cm, respectively, and the calculated figure of merit of the unsaturated absorption (M_a) is approximately 91.2%, indicating that TYDSF has a relatively high conversion efficiency for the pump light at 1610 nm.

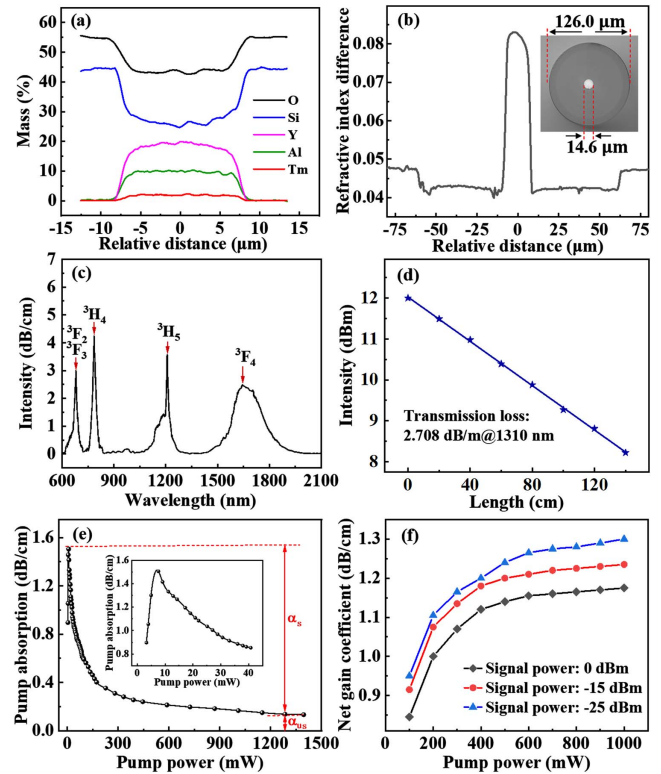


Fig. 1. (a) Element distribution curve along the diameter of TYDSF. (b) The refractive index distribution of TYDSF and the inset is the cross-sectional view. (c) Absorption spectrum. (d) The transmission loss of TYDSF at 1310 nm. (e) Unsaturated absorption at 1610 nm. (f) The gain efficient at different signal powers as a function of pump power.

In order to evaluate the potential of laser performance, the gain coefficients of the TYDSF were measured using the forward pump method with a homemade signal laser at 1944 nm under different 1610 nm pump powers, as presented in Fig. 1(f). The amplification experimental system employed a 2 cm TYDSF as the gain medium at three signal powers: -25 , -15 , and 0 dBm. With the increase of the signal power, the corresponding gain of the TYDSF decreased. The maximum gain coefficient reached 1.26 dB/cm, which is of great benefit for single-frequency fiber lasers with short-cavity configurations.

The experimental setup of the single-frequency fiber laser (DBR-SFFL) system is illustrated in Fig. 2(a), in which a backward pump scheme was utilized with a 1610 nm pump laser. A single-mode wavelength division multiplexer (WDM) was used to input the pump and output the 1944 nm lasing with an isolator (ISO) to protect against backscattered light. The DBR cavity consisted of a low-reflectivity fiber Bragg grating (LR-FBG), 2-cm-long TYDSF, and a high-reflectivity FBG (HR-FBG). The reflectivities of the LR-FBG and HR-FBG were 65.0% and 99.8%, respectively, with a center wavelength of 1944.3 nm [see Fig. 2(c)]. The diagram of the fusion joint between the TYDSF and the FBGs is shown in Fig. 2(b), where no obvious cracks are observed. The core diameter of the FBGs' fiber is 10 μm and the splicing loss of the SMF and TYDSF was measured to be 0.10 dB using a cut-back method at 1310 nm.

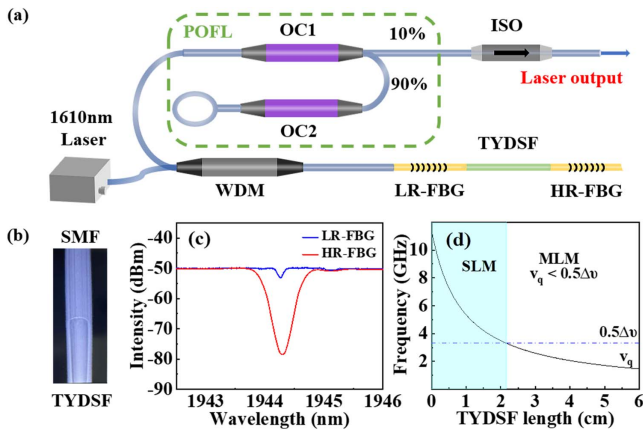


Fig. 2. (a) Experimental setup of the DBR-SFFL and POFL. (b) Fusion point with TYDSF. (c) Transmission spectra of FBG pairs. (d) Calculation for achieving SLM operation.

To achieve SLM operation, it is required that twice the longitudinal mode spacing (ν_q) is more than the reflection bandwidth ($\Delta\nu$). The ν_q is calculated by the equation $c/2nl$, where c is the speed of light, n is the refractive index of the fiber core, and l is the total length of the resonant cavity. The cavity length consists of the length of the TYDSF and the effective lengths of the FBGs (0.87 cm). As shown by the black curve in Fig. 2(d), the ν_q decreases inversely with the length of TYDSF. The 3 dB bandwidth of the LR-FBG is approximately 0.08 nm, and the corresponding $\Delta\nu$ is 6.59 GHz, half of which is 3.29 GHz as shown by the blue dotted line. For the 2-cm-long TYDSF, the calculated ν_q is 3.49 GHz, which is larger than half of the $\Delta\nu$, and thus a SLM laser output at 1944 nm is obtained.

As schematically outlined in the dashed green box in Fig. 2(a), a passive optical feedback loop (POFL) comprising a 10/90 coupler (OC1) and a 50/50 coupler (OC2) was integrated with the DBR-SFFL. The extended cavity formed by the HR-FBG and POFL achieves laser linewidth narrowing through coherent-feedback-induced phase noise suppression^[25]; 90% of the intra-cavity power from OC1 was routed to OC2 to provide optical feedback, while the final laser output was extracted from the 10% port of OC1.

3. Performance of the SFFL

The longitudinal mode characteristic of the DBR-SFFL (without POFL) was measured by the DSH method. The heterodyne signal was analyzed with a photodetector (PD, 5000F, USA) and an electrical spectrum analyzer (ESA, Agilent, USA), revealing a single beating peak at 100 MHz in Fig. 3(a). The absence of mode-hopping sidebands confirms stable SLM operation under these conditions.

The output power characteristics of the DBR-SFFL were investigated with a power meter (PM100D, Thorlabs, USA). As shown in Fig. 3(b), beyond the lasing threshold of 21 mW, the output power scaled linearly with pump power,

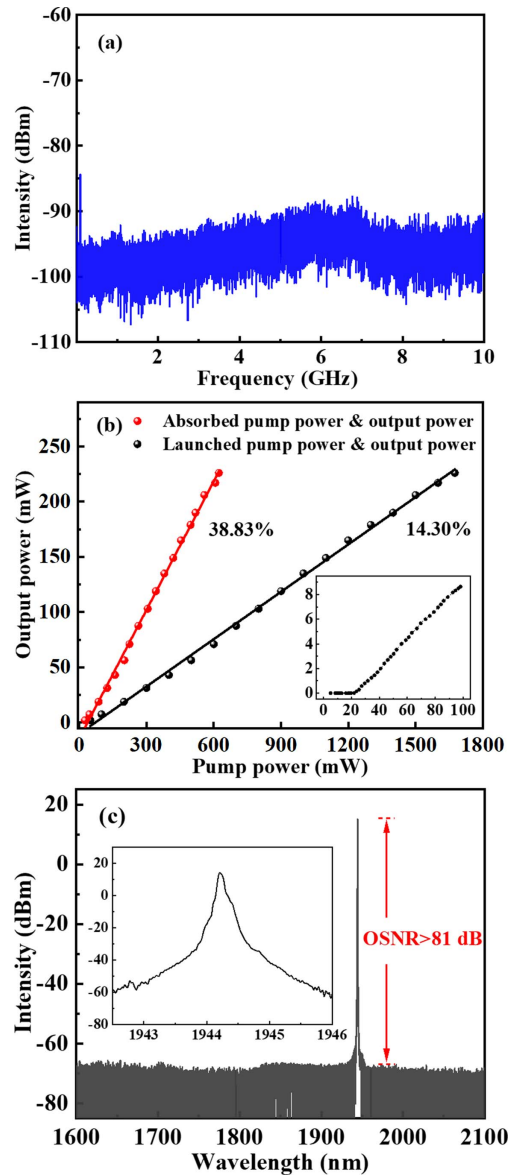


Fig. 3. (a) Radio frequency beating intensity of the DBR-SFFL. (b) Output power of the SFFL as a function of pump power, and the inset is an enlarged view of the graph for a pump power range of 0 to 100 mW. (c) Output spectrum of the SFFL under the maximum output power.

yielding a slope efficiency of 14.30%. A maximum output power of 226 mW was achieved at a launched pump power of 1675 mW. However, the 2-cm-long TYDSF exhibits limited pump absorption efficiency at high power levels. Upon removing the residual pump, the optical-to-optical conversion efficiency defined as output power versus absorbed pump power reached 38.83%. The absence of power saturation suggests potential for further power scaling with higher pump intensities. The output spectrum of the DBR-SFFL is presented in Fig. 3(c), where the inset shows the enlarged region of 1942.5 to 1946.0 nm. A strong narrow-bandwidth lasing peak is centered at 1944.3 nm, the OSNR of which was measured to be 81.5 dB.

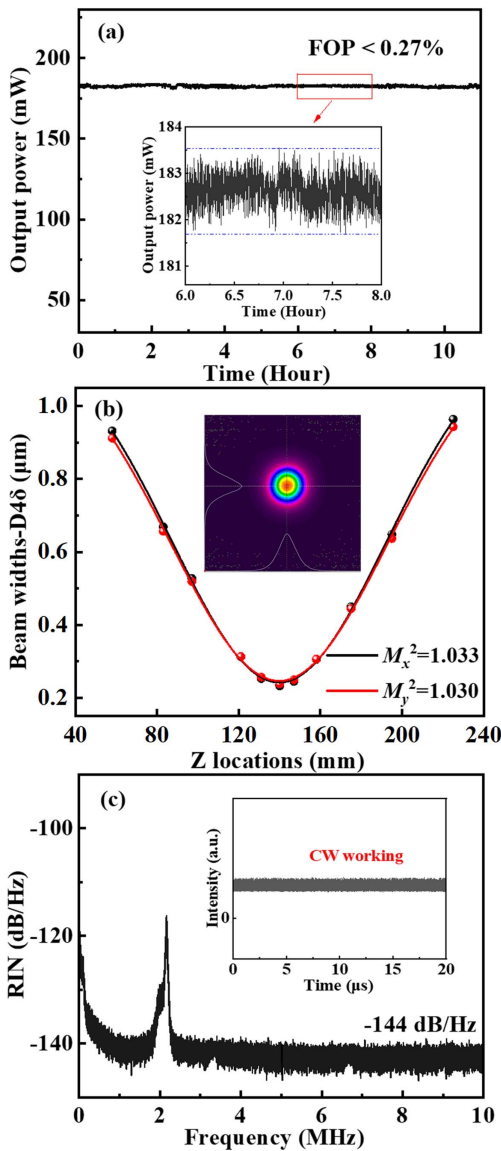


Fig. 4. (a) Laser stability recorded in 11 h. (b) Beam quality and its two-dimensional beam profile. (c) Relative intensity noise and the laser output power dependent on time measured by an oscilloscope.

As shown in Fig. 4(a), the power stability was monitored continuously for every 1 s in 11 h at an output power of ~ 183 mW, and the inset shows an enlarged view within 2 h. The fluctuation of the output power (FOP) is less than 0.27% of the averaged output power. The fluctuations in the output power are attributed to the variations of the pump power and the perturbations of the ambient temperature. The beam quality was characterized using a beam squared system (SP90405, Spiricon, USA), as shown in Fig. 4(b). The quality factors of the laser beam were measured to be 1.033 in the horizontal direction and 1.030 in the vertical direction. The two-dimensional beam profile, as illustrated in the inset, exhibits a close resemblance to the standard Gaussian distribution.

The relative intensity noise (RIN) of the DBR-SFFL was characterized from 10 Hz to 10 MHz with a PD and an ESA at the

maximum output power. Figure 4(c) reveals a relaxation oscillation peak at 2.17 MHz, with RIN stabilizing at -144 dB/Hz beyond 3 MHz. The inset displays the time-domain characteristics observed on an oscilloscope, indicating the SFFL operates in continuous-wave (CW) operation.

The DSH method is unsuitable for characterizing a 1944 nm laser linewidth due to excessive transmission losses. Instead, the beat-frequency method was employed by analyzing heterodyne signals between the BTFL and the SFFL. The pump laser's phase noise is significantly suppressed via acoustic damping and cavity feedback^[26], transferring its stabilized noise profile to the Stokes wave. Consequently, the BTFL frequency closely aligns with the test laser while exhibiting a substantially narrower linewidth,

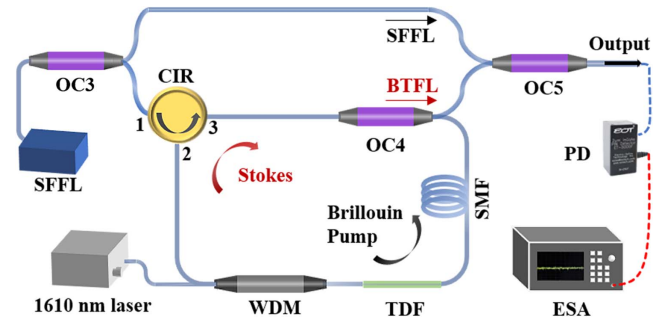


Fig. 5. Linewidth measurement system based on BTFL.

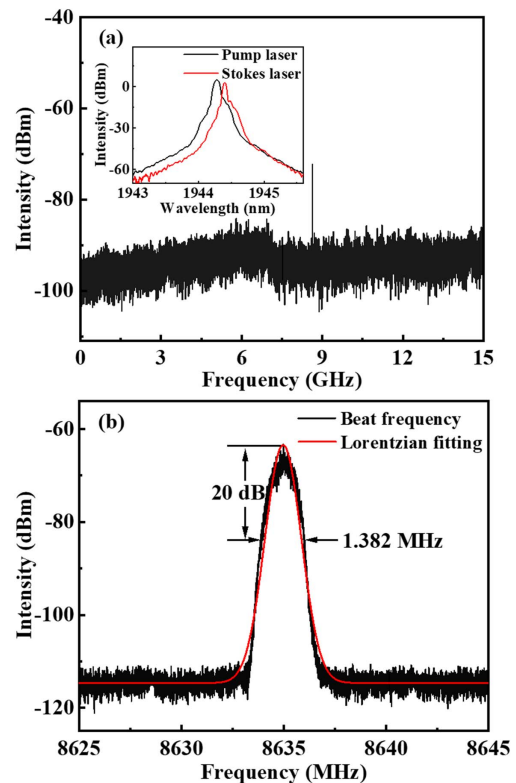


Fig. 6. (a) RF beating spectra and the inset is the optical spectra of the Brillouin pump and Stokes lasers. (b) The linewidth characteristics of the DBR SFFL.

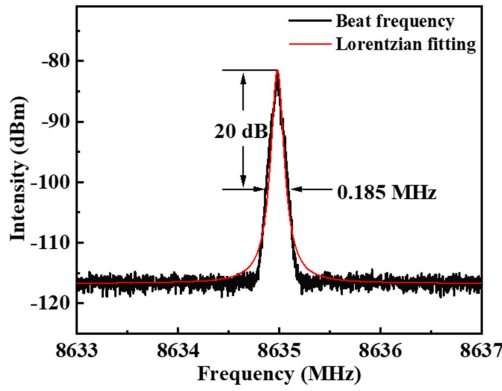


Fig. 7. Linewidth characteristics of the POFL-SFFL.

fulfilling the reference laser criteria for beat-frequency linewidth measurement^[27]. Moreover, the BTFL’s lower Brillouin threshold compared to conventional Brillouin fiber lasers^[22] enables simplified experimental implementation.

Theoretically, the relationship between the linewidth of the Brillouin laser ($\Delta\nu_B$) and that of the pump laser ($\Delta\nu_P$) can be characterized by^[10,22,26,27]

$$\Delta\nu_B = \Delta\nu_P / \kappa^2. \quad (1)$$

The linewidth compression factor κ can be expressed as

$$\kappa = 1 + \frac{\pi n L \Delta\nu_S}{-c \ln R}, \quad (2)$$

where $\Delta\nu_S$ is the Brillouin gain bandwidth, L is the length of the laser cavity, and R is the recoupling coefficient of the laser cavity.

As illustrated in Fig. 5, the linewidth measurement system utilizes a BTFL. The SFFL was split by a fiber coupler (OC3), with

1% routed as the test laser and 99% serving as the BTFL pump source. The pump light entered the ring Stokes cavity via port 1 of an optical circulator (CIR). A 0.2-m-long thulium-doped fiber (TDF) amplified the counter-propagating Brillouin pump and co-propagating Stokes waves, while an 8-m-long SMF acted as the Brillouin gain medium. The BTFL output was extracted from the 1% port of a coupler (OC4). The 11-m-long cavity yielded a longitudinal mode spacing of 18.7 MHz. Given the Brillouin gain bandwidth of 15.0 MHz^[21], the longitudinal mode spacing exceeded the gain bandwidth, ensuring SLM operation. The inset displays the Brillouin pump (1944.28 nm) and Stokes laser (1944.39 nm) spectra, corresponding to a Brillouin frequency shift of 0.11 nm (8.635 GHz).

The BTFL, serving as the reference laser, was combined with the 1% test laser from OC3 via a coupler, OC5 (50:50), to generate the required radio frequency (RF), which was subsequently fed into a PD and an ESA for characterization. The factor κ was calculated to be 7.9 from Eq. (2), indicating that the linewidth of the reference laser is approximately 1/62 that of the test laser. Consequently, the linewidth of the SFFL under test could be directly determined by analyzing the beat signal.

A single beat signal is observed exclusively at 8.635 GHz in Fig. 6(a), which provides robust experimental validation of stable SLM operation in the DBR-SFFL. Figure 6(b) displays the measured RF spectra and the corresponding Lorentzian fitting curve. The 20 dB bandwidth was 1.38 MHz, meaning that the linewidth of the DBR-SFFL was 69.14 kHz. The relatively broad linewidth of the SFFL may be attributed to thermal instability induced by splicing loss and optical-mode-field mismatch at the intracavity fusion splice points^[25,28].

When a POFL was integrated externally to the SFFL cavity, the linewidth measurement in Fig. 7 reveals a laser linewidth of 9.25 kHz, which is significantly narrower than that of the DBR-SFFL. This linewidth narrowing can be attributed to

Table 1. Performance of DBR SFFLs Based on Different Tm-Doped Fibers.

Fiber type	Gain fiber length (cm)	Threshold (mW)	Slope efficiency (%)	Maximum output (mW)	OSNR (dB)	RIN (dB/Hz)	Linewidth (kHz)	Ref.
Tm-doped silica fiber	1.9	75	13.40	18	—	−150	~99.0 ^a	[29]
	1.8	250	9.10	50	65	−150	~36.0 ^a	[30]
Tm-doped germanate fiber	2.1	150	24.70	103	72	−135	~1.65 ^b /~6.0 ^c	[13]
Tm: YAG ceramic fiber	2.0	15	10.20	135	77	−140	~4.5 ^d	[17]
TYDSF-1	1.6	45	50.83	1030	66.5	−139	~40.75 ^a	[18]
TYDSF-2	2.0	21	38.83	226	81	−144	~69.14/ ~9.25 ^d	This work

^aDelayed self-heterodyne method with 10 km SMF.

^bDelayed self-heterodyne method with 3 km SMF.

^cImbalance Michelson fiber interferometer.

^dBTFL-based beating-frequency technique.

the coherent-feedback-induced phase noise suppression and the extended photon lifetime enabled by the hybrid cavity design.

Table 1 summarizes the performance of DBR SFFLs for different Tm-doped fibers. Compared to silica fibers, the TYDSF exhibits higher Tm ion doping concentration, enhanced conversion efficiency, and superior output power. However, the DSH with a 10 km SMF delay line yields an OSNR of only $\sim 1/3$ of the test laser due to excessive losses^[29,30], compromising linewidth accuracy. Tm-doped germanate fiber lasers exhibit higher pump thresholds, likely attributed to mode-field mismatch with silica fibers. Reducing the SMF length to 3 km degrades the DSH resolution to 66 kHz^[13]. While TYDSF-1 achieves watt-level output power and >50% slope efficiency, its OSNR is relatively low; the pump threshold power reaches 45 mW resulting from the core mismatch and beam quality being uncharacterized^[18]. As detailed in Table 1, the SFFL in this work demonstrates well-balanced performance in pump threshold, beam quality, OSNR, stability, and linewidth, surpassing conventional counterparts. The beat-frequency technique based on the BTFL offers a robust and accessible method for linewidth characterization of 2 μm band SFFLs.

4. Conclusion

In summary, we fabricated a TYDSF using a melt-in-tube technique on a CO₂-laser-heating drawing tower, with a Tm³⁺ concentration of 2.30% (mass fraction) and a gain coefficient of 1.26 dB/cm. We obtained a stable CW single-transverse and longitudinal-mode laser operating at 1944 nm with a DBR cavity, delivering an output power of 226 mW using only a 2-cm-long TYDSF. Pumped by a 1610 nm laser, the SFFL achieved an optical-to-optical conversion efficiency of nearly 40% with a remarkably low pump threshold of 21 mW, a high OSNR of 81.5 dB, near-diffraction-limited beam quality, a slight FOP of < 0.27% in 11 h, and a RIN stabilized at -144 dB/Hz. Besides, a linewidth measurement system based on a BTFL was constructed to characterize the linewidth of the SFFL for the first time, which is wavelength-independent and universally applicable for measuring narrow-linewidth lasers across the entire 2 μm spectral region. An optical feedback loop was implemented to narrow the laser linewidth, achieving a reduction from 69.14 to 9.25 kHz. The SFFL exhibits exceptional performance in this work, which is applicable in high-precision medical surgery, atmospheric gas detection, and other fields. Furthermore, the BTFL-based beat-frequency technique offers a robust and simplified solution for linewidth characterization of 2 μm band lasers.

Acknowledgements

This work was supported by the National Natural Science Foundation of China (Nos. U24A20312 and 61975113) and the Natural Science Foundation of Shanghai (No. 24ZR1423900).

References

- J. Geng, Q. Wang, Y. Lee, *et al.*, "Development of eye-safe fiber lasers near 2 μm ," *IEEE J. Sel. Top. Quantum Electron.* **20**, 150 (2014).
- F. Gibert, J. Pellegrino, D. Edouart, *et al.*, "2- μm double-pulse single-frequency Tm: fiber laser pumped Ho: YLF laser for a space-borne CO₂ lidar," *Appl. Opt.* **57**, 10370 (2018).
- M. Tendeau, T. D. Mambu, F. Tjandra, *et al.*, "The use of thulium-doped fiber laser (TDFL) 1940 nm as an energy device in liver parenchyma resection, a-pilot-study in Indonesia," *Ann. Med. Surg.* **60**, 491 (2020).
- M. Janeczek, Z. Rybak, A. Lipińska, *et al.*, "Local effects of a 1940 nm thulium-doped fiber laser and a 1470 nm diode laser on the pulmonary parenchyma: an experimental study in a pig model," *Materials* **14**, 5457 (2021).
- H. H. Keo, C. Somma, C. Regli, *et al.*, "Safety, feasibility, and early efficacy of the water-specific 1940-nm laser wavelength for ablation of saphenous incompetence," *J. Vasc. Surg. Cases. Innov. Tech.* **9**, 101125 (2023).
- X. Cen, X. Guan, C. Yang, *et al.*, "Short-wavelength, in-band-pumped single-frequency DBR Tm³⁺-doped germanate fiber laser at 1.7 μm ," *IEEE Photonics Technol. Lett.* **33**, 350 (2021).
- W. Walasik, D. Traoré, A. Amavigan, *et al.*, "2- μm narrow linewidth all-fiber DFB fiber Bragg grating lasers for Ho- and Tm-doped fiber-amplifier applications," *J. Lightwave Technol.* **39**, 5096 (2021).
- C. Shi, P. Jiang, S. Fu, *et al.*, "1.2 W single-frequency Tm³⁺/Ho³⁺ co-doped fiber oscillator at 2050 nm," *Opt. Lett.* **48**, 6144 (2023).
- T. Yin, Y. Song, X. Jiang, *et al.*, "400 mW narrow linewidth single-frequency fiber ring cavity laser in 2 μm waveband," *Opt. Express* **27**, 15794 (2019).
- D. Li, S. Guo, T. Feng, *et al.*, "2- μm -band single-frequency Tm/Ho co-doped fiber laser with several-kHz linewidth in ~ 100 nm wavelength-tunable range," *Opt. Laser Technol.* **167**, 109766 (2023).
- C. Spiegelberg, J. Geng, Y. Hu, *et al.*, "Low-noise narrow-linewidth fiber laser at 1550 nm," *J. Lightwave Technol.* **22**, 57 (2004).
- Y. Shi, M. Zhang, K. Chen, *et al.*, "Tm³⁺/Ho³⁺ co-doped tellurate glass with high emission cross section for 2 μm fiber lasers," *J. Non-Cryst. Solids* **606**, 122200 (2023).
- Q. Yang, S. Xu, C. Li, *et al.*, "A single-frequency linearly polarized fiber laser using a newly developed heavily Tm³⁺-doped germanate glass fiber at 1.95 μm ," *Chin. Phys. Lett.* **32**, 094206 (2015).
- Y. Wan, J. Wen, C. Jiang, *et al.*, "Over 255 mW single-frequency fiber laser with high slope efficiency and power stability based on an ultrashort Yb-doped crystal-derived silica fiber," *Photonics Res.* **9**, 649 (2021).
- X. Li, J. Wen, Y. Luo, *et al.*, "Over 100 mW linearly polarized single-frequency fiber laser based on Er: YAG crystal-derived silica fiber," *Chin. Opt. Lett.* **22**, 111402 (2024).
- Z. Wei, J. Luan, L. Huang, *et al.*, "Single-frequency fiber laser of 315 mW at 1940 nm based on a Tm: YAG/Ho: YAG-co-derived silica fiber," *Opt. Lett.* **48**, 5109 (2023).
- G. Qian, M. Wu, G. Tang, *et al.*, "Single-frequency distributed Bragg reflector Tm: YAG ceramic derived all-glass fiber laser at 1.95 μm ," *Chin. Phys. B* **31**, 124205 (2022).
- Z. Wei, J. Meng, L. Huang, *et al.*, "Watt-level, high-efficiency single-frequency DBR Tm³⁺-doped YAG crystal-derived silica fiber laser oscillator at 1941 nm," *Opt. Express* **33**, 11944 (2025).
- Y. Bai, F. Yan, T. Feng, *et al.*, "Demonstration of linewidth measurement based on phase noise analysis for a single frequency fiber laser in the 2 μm band," *Laser Phys.* **29**, 075102 (2019).
- D. Yang, F. Yan, T. Feng, *et al.*, "Stable narrow-linewidth single-longitudinal-mode thulium-doped fiber laser by exploiting double-coupler-based double-ring filter," *Infrared Phys. Technol.* **129**, 104568 (2023).
- Y. Luo, Y. Tang, J. Yang, *et al.*, "High signal-to-noise ratio, single-frequency 2 μm Brillouin fiber laser," *Opt. Lett.* **39**, 2626 (2014).
- S. Fu, W. Shi, H. Zhang, *et al.*, "Linewidth-narrowed, linear-polarized single-frequency thulium-doped fiber laser based on stimulated Brillouin scattering effect," *IEEE Photonics J.* **9**, 1 (2017).
- C. Shi, Q. Sheng, S. Fu, *et al.*, "Power scaling and spectral linewidth suppression of hybrid Brillouin/thulium fiber laser," *Opt. Express* **28**, 2948 (2020).
- Q. Zhao, Y. Luo, Q. Hao, *et al.*, "Electron beam irradiation and thermal-induced effects on the spectral properties of BAC-Al in Bi/Er codoped aluminosilicate fibers," *Opt. Mater. Express* **9**, 4287 (2019).

25. Y. Hou, Q. Zhang, and P. Wang, "Frequency-and intensity-noise suppression in Yb³⁺-doped single-frequency fiber laser by a passive optical-feedback loop," *Opt. Express* **24**, 12991 (2016).
26. A. Debut, S. Randoux, and J. Zemmouri, "Linewidth narrowing in Brillouin lasers: theoretical analysis," *Phys. Rev. A* **62**, 023803 (2000).
27. C. Shi, Q. Sheng, S. Fu, *et al.*, "Power scaling and spectral linewidth suppression of hybrid Brillouin/thulium fiber laser," *Opt. Express* **28**, 2948 (2020).
28. G. Agrawal, "Line narrowing in a single-mode injection laser due to external optical feedback," *IEEE J. Quantum Electron.* **20**, 468 (1984).
29. S. Fu, W. Shi, J. Lin, *et al.*, "Single-frequency fiber laser at 1950 nm based on thulium-doped silica fiber," *Opt. Lett.* **40**, 5283 (2015).
30. S. Fu, W. Shi, Q. Sheng, *et al.*, "Compact hundred-mW 2 μ m single-frequency thulium-doped silica fiber laser," *IEEE Photonics Technol. Lett.* **29**, 853 (2017).